

Probing top-Higgs non-standard interactions at the LHC

C. Degrande^{a,b}, J.-M. Gérard^b, C. Grojean^c, F. Maltoni^b, G. Servant^{c,d}

^a*Department of Physics, University of Illinois at Urbana-Champaign, 1110 W. Green Street, Urbana, IL 61801*

^b*Centre for Cosmology, Particle Physics and Phenomenology (CP3)
Chemin du Cyclotron 2, Université catholique de Louvain, Belgium,*

^c*CERN Physics Department, Theory Division, CH-1211 Geneva 23, Switzerland*

^d*Institut de Physique Théorique, CEA/Saclay, F-91191 Gif-sur-Yvette Cédex, France*

Effective interactions involving both the top quark and the Higgs field are among the least constrained of all possible (gauge invariant) dimension-six operators in the Standard Model. Such a handful of operators, in particular the top quark chromomagnetic dipole moment, might encapsulate signs of the new physics responsible for electroweak symmetry breaking. In this work, we compute the contributions of these operators to inclusive Higgs and $t\bar{t}h$ production. We argue that: i) rather strong constraints on the overall size of these operators can already be obtained from the current limits/evidence on Higgs production at the LHC; ii) $t\bar{t}h$ production will provide further key information that is complementary to $t\bar{t}$ measurements, and the possibility of discriminating among different contributions by performing accurate measurements of total and differential rates.

I. INTRODUCTION

The Standard Model (SM) has been tested with an impressive accuracy and is so far in excellent agreement with the experimental data. The room left for new physics at the TeV scale is therefore getting more and more squeezed, thanks to the LHC. Effective field theory (EFT) provides a model independent parametrization of the potential deviations from the SM while keeping its successes if the new degrees of freedom are heavy. EFT has been intensively used for instance in flavor physics to translate the accuracy of the measurements into strong constraints on the coefficients of the associated operators [1]. Slightly softer constraints on the operators involving weak bosons have also been derived from the electroweak precision measurements [2, 3]. In comparison, the operators involving the top quark are poorly constrained so far [4], especially the chromomagnetic moment operator of the top quark [5, 6], while those involving the Higgs field remain largely unconstrained. However, this status is about to change. In particular, modifications of the top quark interactions can significantly change the main Higgs production mechanism at hadron colliders, which is under scrutiny at the LHC.

In this paper, we focus on operators that involve both the top quark and the Higgs field. Not only they are little tested, but it is also where one might expect new physics associated with electroweak symmetry breaking to show up. First, we compute their contributions to $gg \rightarrow h$ due to a top loop. The only non-trivial contribution due to the chromomagnetic operator is logarithmic divergent and can be as large as the SM one. We then derive the constraints from the experimental bound on the Higgs production rate. Higgs production by gluon fusion alone does not allow to distinguish the new contributions since they are all proportional to the SM amplitude. In Section IV, we argue that $t\bar{t}h$ production can provide complementary information to further constrain and to disentangle the various top-Higgs operators.

II. OPERATORS OF INTEREST

Recently, constraints on effective Higgs interactions from the latest Higgs searches have been derived [7–13], with an emphasis on the $d = 6$ operators built from the Higgs and SM gauge bosons. These papers display global fits in a large parameter space. While Ref. [8] and Ref. [9], are restricted to a particular UV set-up where only a sub-class of operators are important, Refs. [7, 10] included the modification of all Higgs interactions to the SM particles but considered that only the Yukawa coupling of the fermions were changed, and therefore have not considered the chromomagnetic operator. The spirit of this work is different in that our motivation is to focus only on $d = 6$ operators that involve both the Higgs field and the top quark. We study their effect on Higgs production by gluon fusion and associated with a $t\bar{t}$ pair, assuming in particular that hWW and hZZ tree-level couplings are not affected by new physics. The results of our analysis can easily be updated once the hWW and hZZ couplings are better determined. We start with the effective lagrangian [14–16]

$$\mathcal{L} = \mathcal{L}^{SM} + \sum \frac{c_i}{\Lambda^2} \mathcal{O}_i + \mathcal{O}\left(\frac{1}{\Lambda^4}\right). \quad (1)$$

The chromomagnetic dipole moment operator modifies the interactions between the gluons and the top quark,

$$\mathcal{O}_{hg} = (\bar{Q}_L H) \sigma^{\mu\nu} T^a t_R G_{\mu\nu}^a, \quad (2)$$

where $\sigma^{\mu\nu} = \frac{i}{2} [\gamma^\mu, \gamma^\nu]$ and T^a is such that $\text{Tr}(T^a T^b) = \delta^{ab}/2$. Besides, one operator contains the top density

$$\mathcal{O}_{Hy} = H^\dagger H (H \bar{Q}_L) t_R \quad (3)$$

and three operators can be built from the top and Higgs currents,

$$\begin{aligned} \mathcal{O}_{Ht} &= H^\dagger D_\mu H \bar{t}_R \gamma^\mu t_R \\ \mathcal{O}_{HQ} &= H^\dagger D_\mu H \bar{Q}_L \gamma^\mu Q_L \\ \mathcal{O}_{HQ}^{(3)} &= H^\dagger \sigma^I D_\mu H \bar{Q}_L \sigma^I \gamma^\mu Q_L. \end{aligned} \quad (4)$$

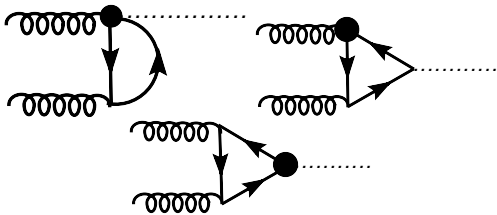


FIG. 1: $gg \rightarrow h$ production. The first two diagrams are the contributions to \mathcal{O}_{HG} from \mathcal{O}_{hg} . The third one is induced by \mathcal{O}_{Hy} and \mathcal{O}_H . The operators of Eq. (4) do not contribute to \mathcal{O}_{HG} (see Sec. III).

Other operators of dimension 6 play a role in the top-Higgs interaction even though they do not contain both fields. One of them is

$$\mathcal{O}_H = \partial_\mu (H^\dagger H) \partial^\mu (H^\dagger H), \quad (5)$$

which amounts to an overall renormalization of the Higgs wave function and therefore to a trivial shift of the top-quark Yukawa coupling [17].

The corrections from those operators to Higgs production by gluon fusion are shown in Fig. 1. In the large top mass limit, the contribution of the operators in Eqs. (2,3) can be seen as corrections to the \mathcal{O}_{HG} operator

$$\mathcal{O}_{HG} = \frac{1}{2} H^\dagger H G_{\mu\nu}^a G_a^{\mu\nu} \quad (6)$$

generated by the scale anomaly. Therefore, we are going to derive the constraints on \mathcal{O}_{HG} from Higgs production, which we will then re-express in terms of limits on a combination of the above operators.

One should remark that not only the Higgs production rate is sensitive to the modifications of the top interactions but also the $h \rightarrow \gamma\gamma$ decay. The operator \mathcal{O}_H does not change the branching ratios since it multiplies all partial widths by the same factor. However, \mathcal{O}_{Hy} and the electromagnetic version of \mathcal{O}_{hg} induce

$$\mathcal{O}_{H\gamma} = \frac{1}{2} H^\dagger H F_{\mu\nu} F^{\mu\nu}. \quad (7)$$

The main effect of this operator will be to relax the constraints from the $h \rightarrow \gamma\gamma$ channel. We reiterate that we do not consider corrections to hWW and hZZ vertices. New top interactions affect all these channels at one-loop. However, their effects to the loop-induced processes $h \rightarrow \gamma\gamma$ and $gg \rightarrow h$ are expected to be relatively larger than for $h \rightarrow WW$ and $h \rightarrow ZZ$ because the new operators modify the SM leading order in the first case and the NLO corrections in the second.

III. HIGGS PRODUCTION BY GLUON FUSION

\mathcal{O}_{HG} is the only dimension-six operator inducing Higgs production by gluon fusion at tree-level. Its effect on the

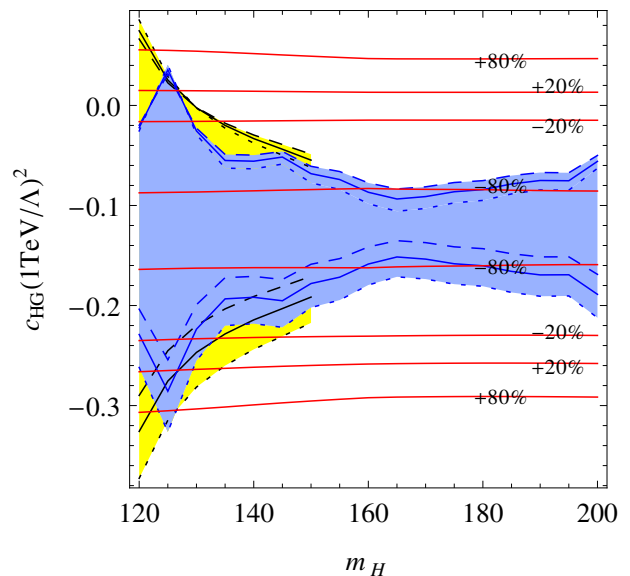


FIG. 2: Region allowed at 95% C.L. by the ATLAS upper bound on the Higgs production cross-section [23] for $\mu_R = \mu_F = m_H/2$ (solid line). The errors are estimated by varying the renormalization and factorization scales from $\mu_R = \mu_F = m_H/4$ (dotted line) to $\mu_R = \mu_F = m_H$ (dashed line). The blue region uses the combination of all channels. The yellow region is obtained using the strongest constraint among the WW and ZZ channels. The red lines show the relative deviation compared to the SM Higgs production rate.

partonic cross-section is (see also Refs. [18, 19])

$$\sigma(gg \rightarrow h) = \sigma(gg \rightarrow h)_{SM} \left(1 + \frac{c_{HG}}{\Lambda^2} \frac{6\pi v^2}{\alpha_s} \right)^2, \quad (8)$$

where we have taken the heavy top limit for the SM, i.e., $m_t > m_H/2$, and $v \approx 246$ GeV is the Higgs vacuum expectation value (vev). The contribution from \mathcal{O}_{HG} is quite large compared to the SM one ($6\pi v^2/\alpha_s \sim 10 \text{ TeV}^2$) because the latter is only generated at the loop-level. Consequently, the upper limits on the Higgs production cross-section from the Tevatron [20] and the LHC [21–23] strongly constrain the allowed range for c_{HG} , as shown on Fig. 2. For this figure, we assume that only \mathcal{O}_{HG} is added to the SM Lagrangian, i.e., we neglect the modifications of the other production mechanisms or of the decay widths except for $h \rightarrow gg$. We used the same NNLO K factor for the contribution of the \mathcal{O}_{HG} as for the SM [24] since both amplitudes are the same up to a global factor. The errors on these limits have been estimated by varying simultaneously the renormalization (μ_R) and factorization scales (μ_F) for the SM and the \mathcal{O}_{HG} tree-level contributions. Other theoretical errors are much smaller. For $m_H = 125$ GeV, we obtain $-0.29 \lesssim c_{HG}(\text{TeV}^2/\Lambda^2) \lesssim 0.036$. We also show in yellow how the constraints on c_{HG} are relaxed when including the effect of $\mathcal{O}_{H\gamma}$. The exclusion in the plane $(c_{HG}, c_{H\gamma})$ is shown in Fig. 3. Again, Fig. 2 is valid only for SM hWW and hZZ couplings but a similar plot can

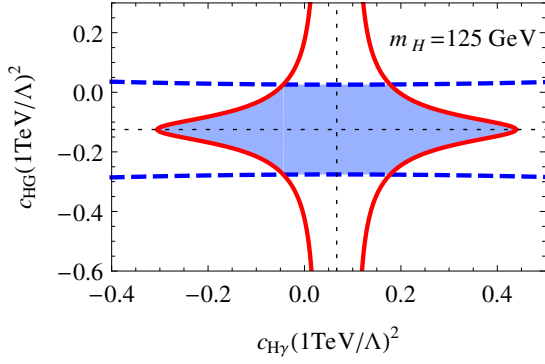


FIG. 3: The dashed blue and solid red lines are the limits from $h \rightarrow (WW, ZZ)$ and $h \rightarrow \gamma\gamma$ respectively. The WW/ZZ constraints on c_{HG} are stronger only when the branching ratio to $\gamma\gamma$ goes below 10^{-3} (SM value), corresponding to $0 \lesssim c_{H\gamma} \lesssim 0.1$. For larger branching ratio, the $\gamma\gamma$ constraints are stronger and do not allow for large values of $c_{H\gamma}$. Note that the allowed region is symmetric along the dotted black lines where $\sigma(gg \rightarrow h) = 0$ and $\Gamma(h \rightarrow \gamma\gamma) = 0$. We have checked that a more refined analysis combining all the channels along the lines of Ref. [9] gives qualitatively similar results, although slightly more constraining of course.

be drawn once the actual values of hWW and hZZ will be determined.

The constraints on c_{HG} of Fig. 2 translate into constraints on a combination of the coefficients of the operators Eqs. (2)–(5). Contrary to the result reported in the first version of our paper as well as in Ref. [25], the one-loop correction from \mathcal{O}_{hg} to the operator \mathcal{O}_{HG} diverges logarithmically in a way consistent with the general expectations from dimension-six operators. Its one-loop contribution can be written as

$$\delta c_{HG} = \frac{g_s y_t}{4\pi^2} \Re c_{hg} \log \left(\frac{\Lambda^2}{m_t^2} \right). \quad (9)$$

The operators \mathcal{O}_{Hy} and \mathcal{O}_H renormalize the top mass

$$m_t = y_t \frac{v}{\sqrt{2}} - \frac{\Re(c_{Hy})}{2\sqrt{2}} \frac{v^3}{\Lambda^2} \quad (10)$$

and/or the top Yukawa coupling,

$$\begin{aligned} \mathcal{L}^{ht\bar{t}} &= \bar{t}t \frac{h}{\sqrt{2}} \left(y_t - \left(\frac{3}{2} \Re(c_{Hy}) + y_t c_H \right) \frac{v^2}{\Lambda^2} \right) \\ &= \bar{t}t h \frac{m_t}{v} \left(1 - c_y \frac{v^2}{\Lambda^2} \right), \end{aligned} \quad (11)$$

where

$$c_y = c_H + \frac{v}{\sqrt{2}m_t} \Re(c_{Hy}). \quad (12)$$

Their contributions are then easily obtained as a simple rescaling of the SM contribution [17, 26]

$$\frac{\delta c_{HG}}{\Lambda^2} = \frac{\alpha_s}{6\pi v^2} \times (-c_y \frac{v^2}{\Lambda^2}). \quad (13)$$

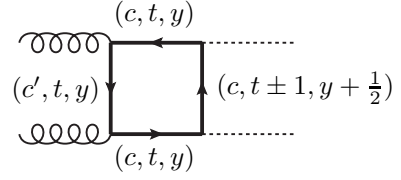


FIG. 4: Diagram leading to the operator \mathcal{O}_{HG} with the particles in the loop labeled by their transformations under $SU(3) \times SU(2) \times U(1)$, i.e., (c, T, Y) if $\bar{c} \otimes c' \ni 8$. If the particles in the loop are bosons, additional diagrams can be obtained by replacing one or two internal lines and their two adjacent vertices by a single vertex.

The other three operators listed in Eq. (4) do not contribute to Higgs production by gluon fusion. In fact, the vertex $ht\bar{t}$ comes from the sum of those operators and of their Hermitian conjugates [40]. The relevant part of the operators can thus be written as

$$\begin{aligned} \partial_\mu (H^\dagger H) \bar{t} \gamma^\mu \gamma_{\pm t} &\propto (H^\dagger H) \partial_\mu \frac{(J_5^\mu \pm J_5^\mu)}{2} \\ &\propto (H^\dagger H) \partial_\mu J_5^\mu \end{aligned} \quad (14)$$

because the vector current is conserved. Their contributions to Higgs production through the effective operator $H^\dagger H G^{\mu\nu} \tilde{G}_{\mu\nu}$, generated by the axial anomaly, vanish in the SM due to parity. This result is consistent with the operator relations derived in Ref. [27]. In Two-Higgs-Doublet-Models with a light pseudo-scalar, this effective operator should be taken into account [28].

Taking $m_t = 174.3$ GeV, $m_H = 125$ GeV, $v = 246$ GeV, $\Lambda = 1$ TeV and $g_s = 1.2$, we obtain

$$\delta c_{HG} \approx 0.1 \Re c_{hg} - 0.006 c_y. \quad (15)$$

Even if the effects due to the new interactions of the top quark are loop suppressed, they cannot be neglected. The coefficient c_y , probing the relation between the top mass and its Yukawa coupling, is not constrained by any other process than Higgs production (see recent and rather weak constraints on $c = 1 - c_y(v/\Lambda)^2$ in

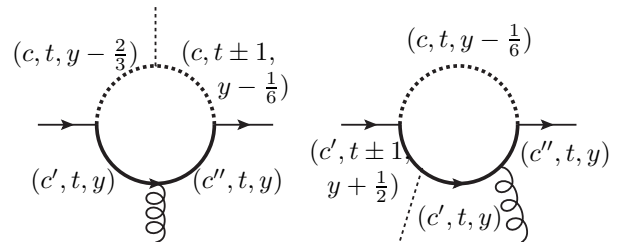


FIG. 5: Diagrams leading to the operator \mathcal{O}_{hg} if $\bar{c}' \otimes c'' \ni 8$, $\bar{c} \otimes c' \ni 3$ and $\bar{c} \otimes c'' \ni 3$. The internal fermion and boson lines can be exchanged and the internal bosons do not have to be scalar. Similarly as for Fig. 4, additional diagrams can be obtained by removing one internal boson propagator.

Refs. [8, 9]). Similarly, the present constraints on c_{hg} due to top pair production [5] including the latest ATLAS combination [29], i.e., $-0.75 \lesssim c_{hg}(\text{TeV}/\Lambda)^2 \lesssim 3$ at 1σ and $-1.2 \lesssim c_{hg}(\text{TeV}/\Lambda)^2 \lesssim 3.5$ at 2σ , still allow the contribution from the chromomagnetic operator to have a noticeable effect on the allowed range for c_{HG} as will be illustrated in the summary plots of Sec. IV.

The next question concerns the typical expectation for the size of the coefficient c_{HG} . For example, the one-loop contributions from \mathcal{O}_H and \mathcal{O}_{Hy} have been shown to be as large as the \mathcal{O}_{HG} contribution in little Higgs models [26]. The reason is that those operators \mathcal{O}_H and \mathcal{O}_{Hy} can be induced by the tree-level exchange of a heavy particle while \mathcal{O}_{HG} is only generated at the loop-level in a perturbative UV completion of the SM (see Fig. 4). The operator \mathcal{O}_H is also enhanced compared to \mathcal{O}_{HG} in strongly interacting Higgs models [17].

On the contrary, the chromomagnetic operator can hardly be enhanced. It is also generated only at the loop-level (see Fig. 5) in perturbation theory and thus for \mathcal{O}_{hg} to be the dominant new physics effects requires \mathcal{O}_{HG} to be relatively suppressed. While the diagram of Fig. 4 can be obtained by using twice the lower part of the second diagram in Fig. 5, the first diagram in Fig. 5 with $c = 1$ does not imply the presence of \mathcal{O}_{HG} . As a consequence, it is possible to generate the chromomagnetic operator, \mathcal{O}_{hg} , at one-loop and not the operator \mathcal{O}_{HG} . An explicit example is given in Appendix A. While dominant in this example, the effects from the chromomagnetic operator are too small to be observed. Alternatively, the hierarchy may come from strongly coupled theories and can be estimated with the help of Naive Dimensional Analysis [30, 31]. If only the right-handed top is strongly coupled, the dominant operator involves four top quarks yet does not contribute even at two-loop [32]. In that case, the coefficient of the chromomagnetic operator is only suppressed by one power of the strong coupling compared to two for c_{HG} and both operators can have similar contribution when the strong coupling approaches 4π . However, its effects may again be too small to be observed. So, let us now move to study the effect of these operators on $t\bar{t}h$ production.

IV. $t\bar{t}h$ PRODUCTION

While both Higgs direct coupling to the gluons and new top interactions significantly affect Higgs production, they cannot be distinguished using this process only. Contrary to Higgs production by gluon fusion, the four operators \mathcal{O}_{HG} , \mathcal{O}_{hg} , \mathcal{O}_H and \mathcal{O}_{Hy} all contribute to $t\bar{t}h$ at the tree-level (see Fig. 6). Again, the three operators in Eq. (4) have no contribution for this process due to parity. There is only one additional operator affecting this process,

$$\mathcal{O}_G = f^{ABC} G_\mu^{A\nu} G_\nu^{B\rho} G_\rho^{C\mu}. \quad (16)$$

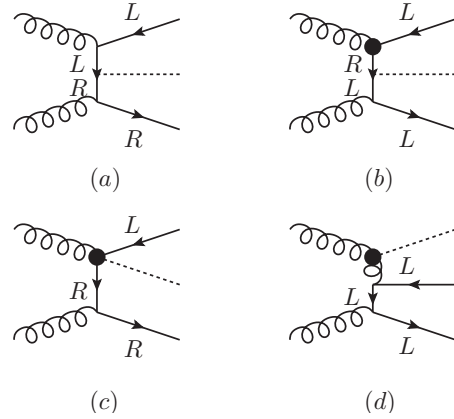


FIG. 6: Examples of diagrams for $t\bar{t}h$ production from the SM (a), from the chromomagnetic operator \mathcal{O}_{hg} (b) and (c) and from the \mathcal{O}_{HG} operator (d). \mathcal{O}_H and \mathcal{O}_{Hy} lead to a simple rescaling of the SM contribution.

However, this operator involves neither the top quark nor the Higgs boson and is thus not expected to be enhanced. Moreover, the interference between \mathcal{O}_G and the SM has a suppression similar to that associated with the octet exchange in top pair production ($\propto \beta^2 m_t^2$) [33]. Indeed, the contribution proportional to c_G in the squared amplitude for $gg \rightarrow t\bar{t}h$ vanishes at threshold and becomes constant at large s . Large shape effects on energy dependent distributions are thus not expected from this operator. Consequently, although we include this operator in the calculation of the cross section, we do not consider it in our phenomenological analysis and set $c_G = 0$ in all plots. The four-fermion operators cannot modify the main process, i.e., gluon fusion. Consequently, their contributions are about one order of magnitude smaller and have not been included. The contribution from \mathcal{O}_H and \mathcal{O}_{Hy} , being just a rescaling of the top Yukawa coupling (see Eqs. (11) and (12)), is proportional to the SM cross section:

$$\sigma(pp \rightarrow t\bar{t}h) = \sigma(pp \rightarrow t\bar{t}h)_{SM} \left(1 - c_y \frac{v^2}{\Lambda^2}\right)^2 \quad (17)$$

and this relation holds at NLO (at least in the flavor universal limit). The total cross-section at 14 TeV is given by

$$\begin{aligned} \frac{\sigma(pp \rightarrow t\bar{t}h)}{\text{fb}} &= 611_{-110}^{+92} + [457_{-91}^{+127} \Re c_{hg} - 49_{-10}^{+15} c_G \\ &+ 147_{-32}^{+55} c_{HG} - 67_{-16}^{+23} c_y] \left(\frac{\text{TeV}}{\Lambda}\right)^2 \\ &+ [543_{-123}^{+143} (\Re c_{hg})^2 + 1132_{-232}^{+323} c_G^2 \\ &+ 85.5_{-21}^{+73} c_{HG}^2 + 2_{-0.5}^{+0.7} c_y^2] \\ &+ 233_{-144}^{+81} \Re c_{hg} c_{HG} - 50_{-14}^{+16} \Re c_{hg} c_y \\ &- 3.2_{-8}^{+8} \Re c_{Hy} c_{HG} - 1.2_{-8}^{+8} c_H c_{HG}] \left(\frac{\text{TeV}}{\Lambda}\right)^4, \end{aligned} \quad (18)$$

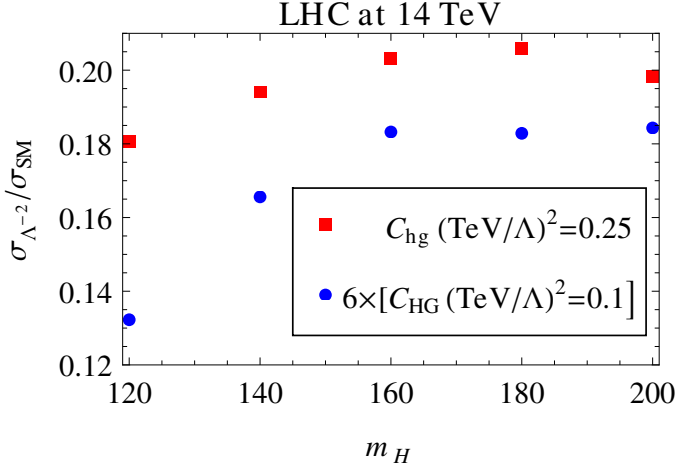


FIG. 7: Ratio of the interference (between the SM and the main dimension-six operators) and the SM $pp \rightarrow t\bar{t}h$ cross section as a function of the Higgs mass. CTEQ6l1 pdf set and $\mu_R = \mu_F = m_t = 174.3$ GeV are used and the results are very similar at 7 TeV.

at 8 TeV by

$$\begin{aligned} \frac{\sigma(pp \rightarrow t\bar{t}h)}{\text{fb}} &= 128 + [94\Re c_{hg} - 9.7c_G + 27c_{HG} \\ &- 15c_y] \left(\frac{\text{TeV}}{\Lambda}\right)^2 + [53.9(\Re c_{hg})^2 + 137c_G^2 \\ &+ 9.6c_{HG}^2 + 0.4c_y^2 + 19.3\Re c_{hg}c_{HG} \\ &- 9.6\Re c_{hg}c_y - 1.2\Re c_{Hy}c_{HG} \\ &- 0.7c_{HC}c_{HG}] \left(\frac{1 \text{ TeV}}{\Lambda}\right)^4, \end{aligned} \quad (19)$$

and at 7 TeV by

$$\begin{aligned} \frac{\sigma(pp \rightarrow t\bar{t}h)}{\text{fb}} &= 86.3_{-15}^{+10} + [63_{-14}^{+20}\Re c_{hg} + 22.3_{-7}^{+8}c_{HG} \\ &- 10.2_{-2.5}^{+4}c_y - 5.6c_G] \left(\frac{\text{TeV}}{\Lambda}\right)^2 \\ &+ [43.6_{-12}^{+17}(\Re c_{hg})^2 + 78.3c_G^2 + 8.6_{-3}^{+1}c_{HG}^2 \\ &+ 0.3c_y^2 + 21_{-2}^{+6}\Re c_{hg}c_{HG} - 7.2_{-1.7}^{+1}\Re c_{hg}c_y \\ &- 1.5_{-1}^{+1}\Re c_{Hy}c_{HG} - 1.1_{-1}^{+1}c_{HC}c_{HG}] \left(\frac{\text{TeV}}{\Lambda}\right)^4, \end{aligned} \quad (20)$$

for $m_H = 125$ GeV. We included c_G and c_G^2 terms for indication (but not $c_G c_i$ terms), however, as mentioned earlier, we will set $c_G = 0$ in the rest of the analysis.

The same factorization and renormalization scales as for top pair production, i.e., $\mu_F = \mu_R = m_t$ have been used since we have only considered a light Higgs boson. The cross-section will slightly decrease if higher values taking into account the Higgs mass are chosen. The errors are again obtained by varying the factorization and renormalization scales simultaneously from $\mu_F = \mu_R = m_t/2$ to $\mu_F = \mu_R = 2m_t$, except for the

last two terms $\Re(c_{Hy})c_{HG}$ and $c_{HC}c_{HG}$ for which the numerical errors are larger. Results have been obtained via the FeynRules-MadGraph 5 simulation chain [34–37]. The new physics has been computed at the tree-level and the SM contribution at NLO [24, 38, 39]. The $\mathcal{O}(1/\Lambda^4)$ terms have been computed to check the $1/\Lambda$ expansion and only take into account the operators that contribute also at the $1/\Lambda^2$ order, i.e., contain either squares of the operators $\mathcal{O}(1/\Lambda^2)$ or the interference of the SM with an amplitude involving two new vertices. Additional contributions from the operators in Eq. (4) or dimension-eight operators and proportional to the imaginary part of c_{Hy} or c_{hg} are not included. The values of the $1/\Lambda^4$ coefficients tell us that the $1/\Lambda$ expansion breaks down around the TeV for $c_i = 1$. This lower value compared to top pair production [5] is expected due to the higher energy required for this final state. While Eqs. (18)–(20) have been obtained only for a particular value of the Higgs mass, the ratios of the new physics contributions over the SM do not change drastically with the Higgs mass as shown on Fig. 7.

As shown by Eqs. (18)–(20) and Fig. 7, $t\bar{t}$ associated Higgs production can mainly be affected by the chromomagnetic operator. As a consequence, the constraints from a measurement of the $t\bar{t}h$ cross-section would complement those from Higgs production as illustrated in Fig. 8, which displays the c_{hg} range allowed by the present measurements of the $t\bar{t}$ cross section. By the time the $t\bar{t}h$ cross section will be measured, the improved constraints from $t\bar{t}$ measurements will also help in reducing further the allowed range for c_{hg} according to Ref. [5]:

$$\delta\sigma_{pp \rightarrow t\bar{t}}|_{14 \text{ TeV}} = 144 c_{hg} \left(\frac{\text{TeV}}{\Lambda}\right)^2 + 22.5 c_{hg}^2 \left(\frac{\text{TeV}}{\Lambda}\right)^4. \quad (21)$$

Like for top pair production, the theoretical uncertainty is responsible for a sizable part of the allowed region. Since those errors mainly affect the overall normalisation, this issue could be solved by measuring the shapes of the distributions. Additionally, shape effects could also lift the remaining degeneracy between the four operators. While the contributions of the operators \mathcal{O}_{Hy} and \mathcal{O}_H have the same shapes as the SM ones, the operators \mathcal{O}_{hg} and \mathcal{O}_{HG} can induce shape distortions. However, only the contribution of the chromomagnetic operator might have a higher energy dependence than the SM. If the Higgs leg is attached to the effective vertex, the diagrams contain only one chirality flip such that no other chirality flip is needed to interfere with the SM amplitude (Fig. 6(c)). Moreover, the vertex is not proportional to the Higgs vev like for top pair production. Those advantages are lost if the Higgs is attached to the top line or to a gluon (Figs. 6(b) and (d)). For those diagrams, the amplitude is proportional to m_t and v and no room is left for extra powers of the energy of the process.

The distributions of the transverse momentum of the Higgs, the total H_T and the invariant mass of the Higgs-top system are displayed on Fig. 9. The shapes of the

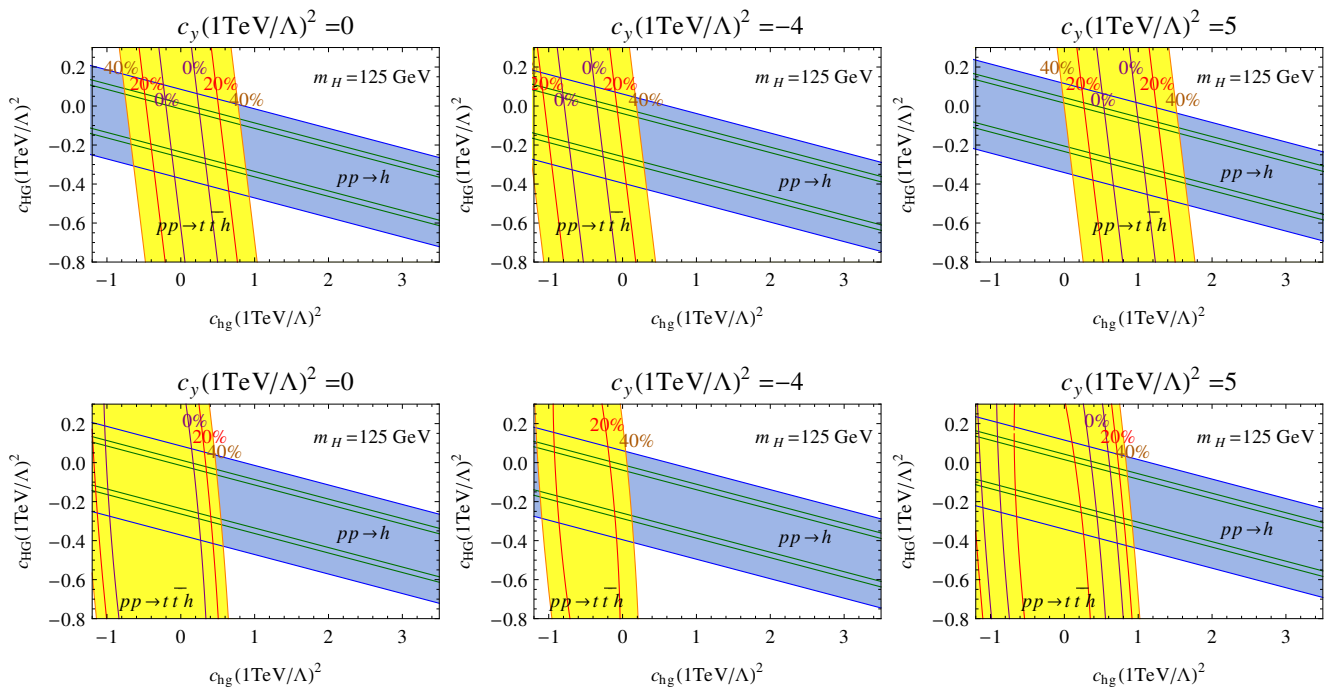


FIG. 8: In blue, the region allowed by the Higgs production constraints at 7 TeV for $m_H = 125$ GeV. The green lines delimit the 2 allowed tiny bands obtained if the Higgs cross-section is measured at its SM value with a precision of 20%. The yellow region is obtained by assuming a 40% precision on the $t\bar{t}h$ cross-section at 14 TeV with the measured central value matching the SM prediction and $c_G = 0$. The three plots correspond respectively to $c_y(\text{TeV}/\Lambda)^2 = 0, -4, +5$. The upper plots are obtained when neglecting the $\mathcal{O}(1/\Lambda^4)$ terms in the $t\bar{t}H$ cross section. The bottom plots instead include these higher order terms.

$1/\Lambda^4$ contributions are also shown for comparison. They are clearly stretched to high energy while the interference and the SM contributions have a very similar behavior. The interference with the diagrams in which the Higgs is connected at the effective vertex do not vanish but are apparently suppressed. The shape effects are only expected if the new physics scale Λ is close to the maximal energy probed because they are due only to the $1/\Lambda^4$ contributions. The plots on the right show how the distributions can differ with respect to the SM in the case $c_{hg}(\text{TeV}^2/\Lambda^2) = 1$.

Finally, spin correlations could exhibit some dependence on c_{hg} . In the case of $t\bar{t}$ production, the deviations due to c_{hg} were of the order of a few percents [5]. For $t\bar{t}h$, the measurement will be much more challenging and we therefore do not compute the associated spin correlations here but might return to them in due time.

V. CONCLUSION

Only one dimension-six operator, \mathcal{O}_{HG} , generates a tree level coupling between the Higgs boson and the gluons. This operator has the largest contribution to Higgs production. Nevertheless, the three operators modifying the contribution from the top loop also have sizable effects compared to the SM one and, in a large

class of models, can be comparable to the effect of \mathcal{O}_{HG} due to the hierarchy between their coefficients. All those operators are already constrained by the present limits on Higgs production at hadron colliders. However, Higgs production by gluon fusion only constrains a linear combination of these operators and cannot discriminate between them. Interestingly, a light Higgs makes real the possibility of partially solving this issue by using Higgs production in association with a pair of top quarks. Contrary to Higgs production, the leading contribution in this process comes from the chromomagnetic operator \mathcal{O}_{hg} , which can therefore be further constrained from the measurement of the total $t\bar{t}h$ cross-section. Shape effects do not come from the interference terms and are dominated by the square of the amplitude involving an effective vertex and could thus be observable for large c_{hg} values only.

Acknowledgments: We would like to thank C. Zhang for pointing out a mistake in our original computation of the one-loop corrections to \mathcal{O}_{HG} . The work of C.D., J.-M. G. and F.M. is supported by the Belgian Federal Office for Scientific, Technical and Cultural Affairs through the Interuniversity Attraction Pole No. P6/11. C.D. is a fellow of the Fonds National de la Recherche Scientifique and the Belgian American Education Foundation. G.S is supported by the ERC

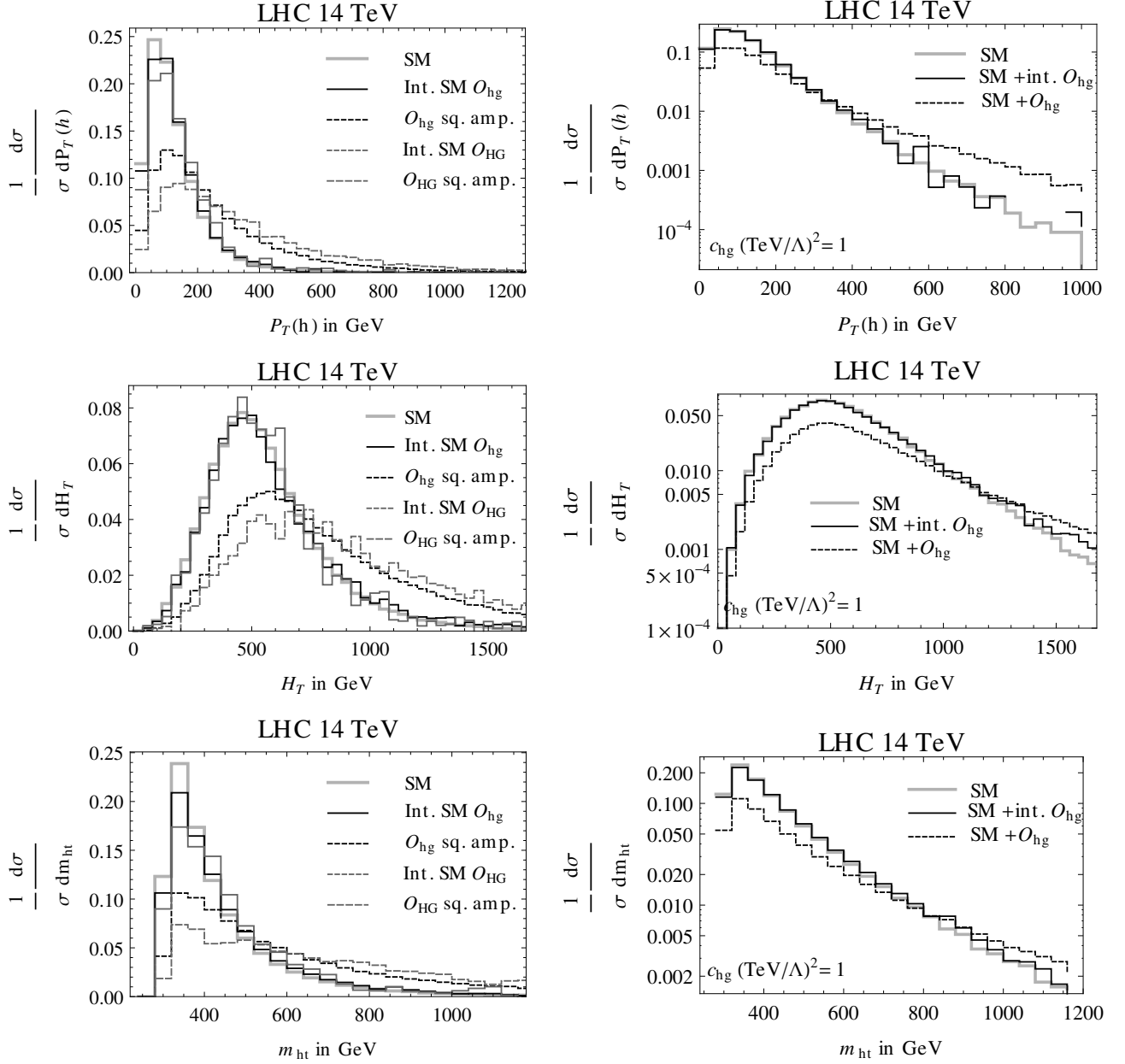


FIG. 9: Left: Normalized distributions of the Higgs transverse momentum $P_T(h)$, the total H_T and the invariant mass of the Higgs-top system using CTEQ611 pdf set, $\mu_R = \mu_F = m_t = 174.3$ GeV and $m_H = 125$ GeV for the SM, its interference with O_{hg} and O_{HG} and the squared of the amplitudes with one effective vertex. These plots do not depend on the value of c_{hg} and c_{HG} . Right: Total contribution (SM + O_{hg}) for $c_{hg}(\text{TeV}/\Lambda)^2 = 1$ including the interference terms only and including both the interference terms and the terms of order $1/\Lambda^4$, compared to the SM only.

Starting Grant 204072. C.G. is partly supported by the European Commission under the ERC Advanced Grant 226371 MassTeV and the contract PITN-GA-2009-237920 UNILHC. We thank D. Choudhury and P. Saha for useful discussions about the contribution of the chromomagnetic operator in $gg \rightarrow h$.

Appendix A: Explicit example with $c_{HG} \ll c_{hg}$

In this appendix, we provide a toy model in which the diagrams of Fig. 5 are generated while the diagram of Fig. 4 is not. The new sector is given by

$$\begin{aligned}
 T_{L,R} &\sim (3, 1, Y) \\
 \Phi &\sim (1, 2, Y - 1/6) \\
 S &\sim (1, 1, Y - 2/3)
 \end{aligned}
 \tag{A1}$$

where $Y \neq 2/3$ to avoid the mixing of T with the SM top and $Y \neq -1/3$ to avoid the mixing between Φ and the Higgs doublet. The extra piece of the Lagrangian is given by

$$\begin{aligned} \mathcal{L}^{NP} = & i\bar{T}\not{\partial}T - M\bar{T}T - \kappa(\bar{T}_R Q_L \Phi + \bar{Q}_L T_R \Phi^\dagger) \\ & -\beta(\bar{t}_R T_L S^\dagger + \bar{T}_L t_R S) + D_\mu S^\dagger D^\mu S - M_S^2 S^\dagger S \\ & +\lambda_1 (S^\dagger S)^2 + \lambda_2 S^\dagger S H^\dagger H + \lambda_3 S^\dagger S \Phi^\dagger \Phi \\ & +D_\mu \Phi^\dagger D^\mu \Phi - M_\Phi^2 \Phi^\dagger \Phi + \lambda_4 (\Phi^\dagger \Phi)^2 \\ & +\lambda_5 \Phi^\dagger \Phi H^\dagger H + M_3 (\Phi^\dagger H^\dagger S + H \Phi S^\dagger) , \quad (\text{A2}) \end{aligned}$$

where the parameters M , M_S , M_Φ and M_3 are around or above the TeV scale. The model has an accidental Z_2 symmetry under which all the SM model particles are even while the new ones are odd. This symmetry prevents any tree-level generation of the higher dimensional operators when the heavy particles are integrated

out. The operator \mathcal{O}_{HG} cannot be generated at one-loop since the colored particle does not couple to the Higgs. On the contrary, the equivalent operator for the photon cannot be avoided. Indeed, even if the fermions can be chosen to be neutral, all the new scalars cannot be simultaneously neutral. The constraints from gluon fusion in the low mass will change with the branching ratio to two photons. Nevertheless, the chromomagnetic operator is induced at one-loop and its coefficient given by

$$\begin{aligned} \frac{c_{hg}}{\Lambda^2} = & \frac{\kappa\beta g_s M_3}{4(4\pi)^2 M^3} \left[\frac{R_\Phi^2 (1 - 3R_S^2) + R_S^2 + 1}{(R_\Phi^2 - 1)^2 (R_S^2 - 1)^2} \right. \\ & \left. + \frac{4 \left(\frac{R_S^4 \log(R_S)}{(R_S^2 - 1)^3} - \frac{R_\Phi^4 \log(R_\Phi)}{(R_\Phi^2 - 1)^3} \right)}{R_\Phi^2 - R_S^2} \right] \quad (\text{A3}) \end{aligned}$$

where $R_S \equiv \frac{M_S}{M}$ and $R_\Phi \equiv \frac{M_\Phi}{M}$.

-
- [1] M. Bona et al. (UTfit Collaboration), JHEP **0803**, 049 (2008), 0707.0636.
- [2] Z. Han and W. Skiba, Phys.Rev. **D71**, 075009 (2005), hep-ph/0412166.
- [3] R. Barbieri, A. Pomarol, R. Rattazzi, and A. Strumia, Nucl.Phys. **B703**, 127 (2004), hep-ph/0405040.
- [4] C. Zhang, N. Greiner, and S. Willenbrock (2012), 1201.6670.
- [5] C. Degrande, J.-M. Gerard, C. Grojean, F. Maltoni, and G. Servant, JHEP **1103**, 125 (2011), 1010.6304.
- [6] J. F. Kamenik, M. Papucci, and A. Weiler (2011), 1107.3143.
- [7] D. Carmi, A. Falkowski, E. Kuflik, and T. Volansky (2012), 1202.3144.
- [8] A. Azatov, R. Contino, and J. Galloway (2012), 1202.3415.
- [9] J. Espinosa, C. Grojean, M. Muhlleitner, and M. Trott (2012), 1202.3697.
- [10] P. P. Giardino, K. Kannike, M. Raidal, and A. Strumia (2012), 1203.4254.
- [11] J. Ellis and T. You (2012), 1204.0464.
- [12] A. Azatov, R. Contino, D. Del Re, J. Galloway, M. Grassi, et al. (2012), 1204.4817.
- [13] M. Farina, C. Grojean, and E. Salvioni (2012), 1205.0011.
- [14] W. Buchmuller and D. Wyler, Nucl.Phys. **B268**, 621 (1986).
- [15] B. Grzadkowski, M. Iskrzynski, M. Misiak, and J. Rosiek, JHEP **10**, 085 (2010), 1008.4884.
- [16] G. Buchalla and O. Cata (2012), 1203.6510.
- [17] G. Giudice, C. Grojean, A. Pomarol, and R. Rattazzi, JHEP **0706**, 045 (2007), hep-ph/0703164.
- [18] A. V. Manohar and M. B. Wise, Phys.Lett. **B636**, 107 (2006), hep-ph/0601212.
- [19] A. Pierce, J. Thaler, and L.-T. Wang, JHEP **0705**, 070 (2007), hep-ph/0609049.
- [20] T. Aaltonen et al. (CDF and D0 Collaboration) (2011), 1103.3233.
- [21] G. Aad et al. (ATLAS Collaboration) (2011), ATLAS-CONF-2011-163.
- [22] S. Chatrchyan et al. (CMS Collaboration) (2011), CMS-PAS-HIG-11-032.
- [23] G. Aad et al. (ATLAS Collaboration), Phys.Lett. **B710**, 49 (2012), 1202.1408.
- [24] S. Dittmaier et al. (LHC Higgs Cross Section Working Group) (2011), 1101.0593.
- [25] D. Choudhury and P. Saha (2012), 1201.4130.
- [26] I. Low and A. Vichi, Phys.Rev. **D84**, 045019 (2011), 1010.2753.
- [27] J. Aguilar-Saavedra, Nucl.Phys. **B821**, 215 (2009), 0904.2387.
- [28] E. Cervero and J.-M. Gerard (2012), 1202.1973.
- [29] G. Aad et al. (ATLAS Collaboration) (2012), <https://twiki.cern.ch/twiki/pub/AtlasPublic/>.
- [30] H. Georgi, Phys.Lett. **B298**, 187 (1993), hep-ph/9207278.
- [31] A. Manohar and H. Georgi, Nucl.Phys. **B234**, 189 (1984).
- [32] D. Nomura, JHEP **1002**, 061 (2010), 0911.1941.
- [33] C. Zhang and S. Willenbrock, Phys.Rev. **D83**, 034006 (2011), 1008.3869.
- [34] N. D. Christensen and C. Duhr, Comput.Phys.Commun. **180**, 1614 (2009), 0806.4194.
- [35] C. Degrande, C. Duhr, B. Fuks, D. Grellscheid, O. Mattelaer, et al. (2011), 1108.2040.
- [36] P. de Aquino, W. Link, F. Maltoni, O. Mattelaer, and T. Stelzer (2011), 1108.2041.
- [37] J. Alwall, M. Herquet, F. Maltoni, O. Mattelaer, and T. Stelzer, JHEP **1106**, 128 (2011), 1106.0522.
- [38] W. Beenakker, S. Dittmaier, M. Kramer, B. Plumper, M. Spira, et al., Phys.Rev.Lett. **87**, 201805 (2001), hep-ph/0107081.
- [39] S. Dawson, L. Orr, L. Reina, and D. Wackerroth, Phys.Rev. **D67**, 071503 (2003), hep-ph/0211438.
- [40] This combination is invariant under custodial symmetry and can thus not be constrained by the ρ parameter.